



## Report on BCM1F Simulation Studies

Qingxin Xia, Tsinghua University, China

September 5, 2013

### Abstract

BCM1F, the Fast Beam Conditions Monitor, is used to monitor the flux of particles with nanosecond time resolution in and around the CMS detector. When LHC restarted running with beams and providing proton-proton collisions, BCM1F has recorded the data of time, luminosity, rate and so on. For further studying, Monte Carlo simulation is used to provide data and analysis to upgrade BCM1F. Luminosity measurement is one aspect to be researched with the simulation. In this article, the hit probability from the simulation is compared with the data from measurement. A method of splitting the sensors is used to reduce the rate for the luminosity measurement.

# Contents

<b>1</b>	<b>Introduction</b>	<b>3</b>
<b>2</b>	<b>Fast Beam Conditions Monitor (BCM1F)</b>	<b>3</b>
2.1	Overview . . . . .	3
2.2	Performance . . . . .	5
2.2.1	Spectra . . . . .	5
2.2.2	Particle Rates . . . . .	5
2.2.3	Luminosity Monitoring . . . . .	8
2.2.4	Time Information . . . . .	8
2.2.5	Albedo Effect . . . . .	8
<b>3</b>	<b>Relevant Physical Quantities in Simulation</b>	<b>8</b>
3.1	Simulated Hits . . . . .	8
3.2	Time of Flight . . . . .	8
3.3	Signal . . . . .	9
3.4	Pile-up . . . . .	9
3.5	Hit Probability . . . . .	9
<b>4</b>	<b>Processing Methods</b>	<b>10</b>
4.1	Simulation Samples . . . . .	10
4.2	Luminosity Algorithms . . . . .	10
4.3	Channel Splitting . . . . .	11
<b>5</b>	<b>Results</b>	<b>12</b>
5.1	Hit Probability . . . . .	12
5.2	Luminosity Algorithms . . . . .	16
5.3	Channel Splitting . . . . .	16
<b>6</b>	<b>Summary and Conclusions</b>	<b>19</b>

# 1 Introduction

The Large Hadron Collider (LHC)[1] has been successfully providing proton-proton collisions since 2009. To monitor the circumstances in the Compact Muon Solenoid (CMS)[2] experiment, some beam conditions and radiation monitors were installed. The CMS Fast Beam Conditions Monitor, BCM1F[3], is one of the subsystems of the CMS Beam Conditions and Radiation Monitoring (BRM)[4] system. It monitors the flux of particles with nanosecond resolution and also gives some other information like time, rate and so on. BCM1F has been recording data from beam-halo and collision particles.

For further upgrading, Monte Carlo simulation is used to provide result and comparison. The simulation is improved by the continuous comparison between the simulated data and the measured data. When the simulation is set nearly to the real circumstances of BCM1F, further monitoring and analysing can be processed even though the experiment do not obtain the rigorous conditions. Then more measures can be done for the upgrading of BCM1F.

Luminosity measurement is very important for physics analyses. Simulations are performed for it after analysing and checking the simulated data. For higher rate conditions there is no data measured but with the simulation luminosity measurement can be processed by some reasonable algorithms.

## 2 Fast Beam Conditions Monitor (BCM1F)

### 2.1 Overview

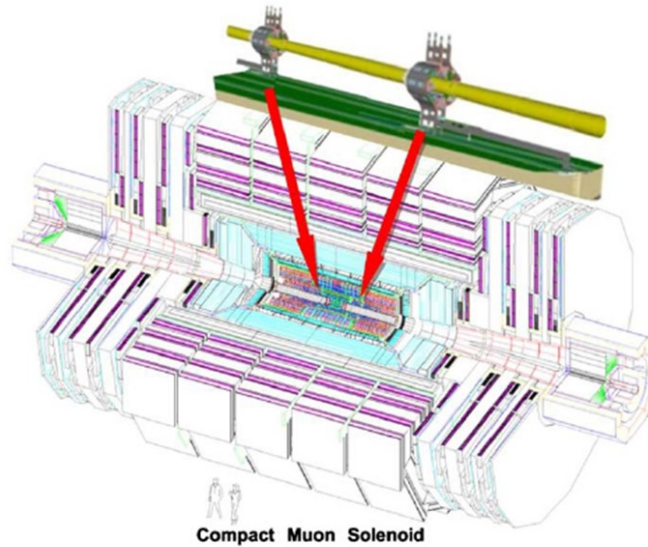


Figure 1: A sketch of the CMS detector showing the location of BCM1F inside the track by the arrows.

The Fast Beam Conditions Monitor, BCM1F, is one among the beam conditions and radiation monitors installed in and around the CMS detector.[5] It is based on single crystal diamonds using chemical vapour deposition techniques. The single crystal chemical vapour deposition (sCVD) diamond sensors have nice radiation hardness because of its large displacement energy and low leakage current with almost no temperature dependence. This kind of character removes the need for active cooling and makes sCVD an attractive material to be used in a particle detector in areas of high radiation dose and in locations where space is limited. In addition, diamond sensors are characterised by fast response allowing time measurements with nanosecond resolution.[6]

Four  $5 \times 5 \times 0.5 \text{ mm}^3$  sCVD diamond sensors are mounted  $\sim 5 \text{ cm}$  radially from the beamline on two planes located on both sides and  $\sim 1.8 \text{ m}$  away from the CMS interaction point (IP), as sketched in Figure 1. For the edges hits usually cannot be recorded, so the effective size of the sensors is  $4.7 \times 4.7 \times 0.5 \text{ mm}^3$ .

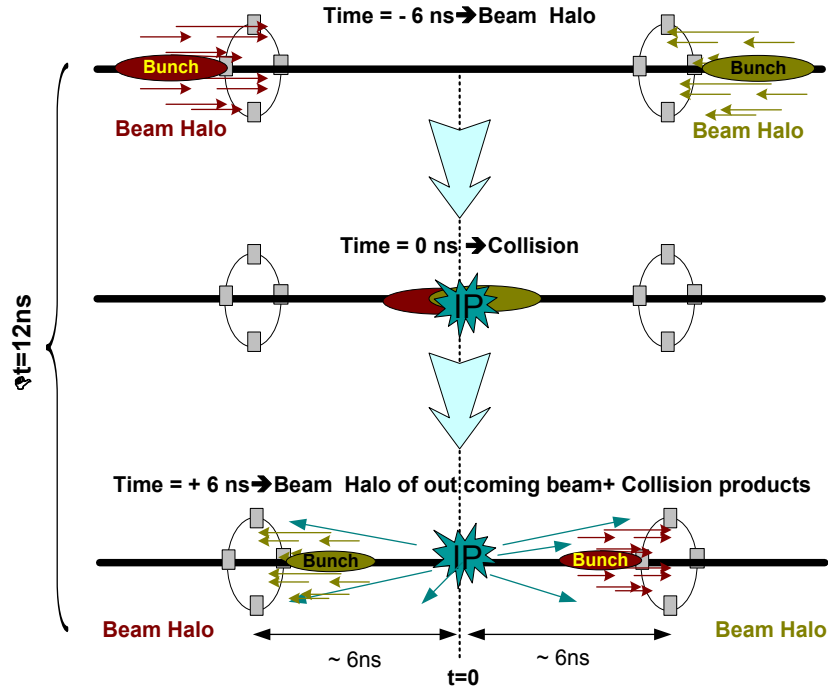


Figure 2: Time scheme of a bunch crossing in the IP.

The distance between the sensors and the IP is optimal for the separation of incoming and outgoing particles and corresponds to a flight time of about 6 ns for relativistic particles (Figure 2).

Each sensor is connected to a radiation-hard front-end electronics where the signals are pre-amplified and transmitted as an analogue optical signal with an optical driver. The signals are converted back to electrical signals at the back-end and then processed by a system made up of scalers, look-up table (LUT), flash analogue-to-digital converters (ADCs) and time-to-digital converters (TDCs), which provides the information on hit

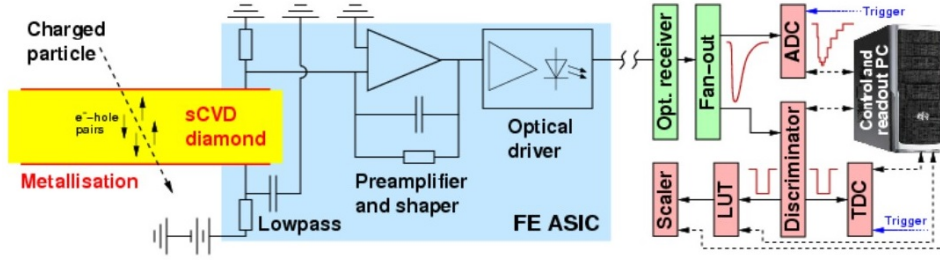


Figure 3: The readout chain of BCM1F.

rates, coincidences, signal shape, time over an orbit and so on. The readout chain of BCM1F is shown in Figure 3.

## 2.2 Performance

### 2.2.1 Spectra

A typical hit signal digitised by the ADCs shows the baseline and the pulse height, as sketched in Figure 4. The spectrum of the signal pulse height from proton-proton collision products, from one of the diamond sensors, is shown in Figure 5. In the signal region of the spectrum, which lies from the threshold of the discriminator to the saturation of the front-end, the first maximum is identified as the height corresponding to minimum ionising particles (MIP). Limitation of the front-end electronics yields another peak at  $\sim 10$  MIPs that is caused by saturation. The thresholds used to discriminate the signals fed into scalers, the LUT and the TDCs are adjusted to be the value at the minimum between the pedestal and the MIP maximum. The monitoring of the pulse height spectra is very important, for example to assess degradation of the signal due to radiation damage mainly to the laser.

### 2.2.2 Particle Rates

The discriminated signals of each channel are input into a CAEN V260 scaler where they are counted and then the hit rate is provided. Hit rates from BCM1F are very sensitive to variations of the beam conditions, such as when the machine operators take an action. The rates during an LHC fill is shown in Figure 6, where the different steps of the fill can be well characterised. Before any beam is in the machine, the rates are essentially from noise and cosmic, and possibly from de-activation of the material in the vicinity of BCM1F. As beams are injected and accelerated, the increase in the rates is observed and found out to be essentially from beam-gas interactions due to an increase of the vacuum pressure. The vacuum pressure stabilises during the flat-top procedure and the rate is constant. The rate jumps orders of magnitude when the collisions start. Finally the rate drops exponentially after the beams are dumped.

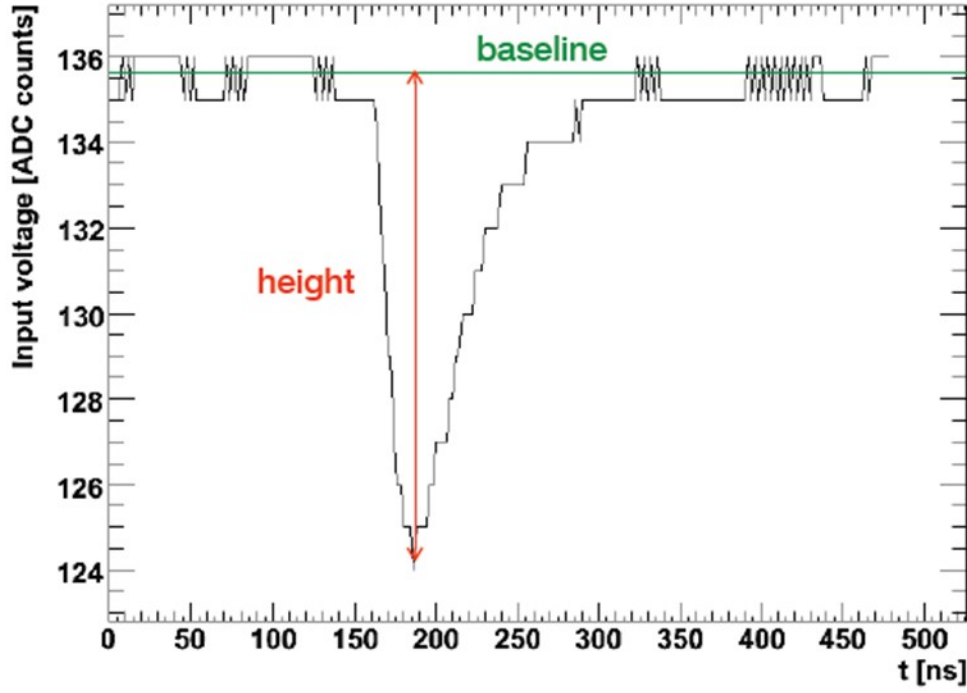


Figure 4: A typical hit signal digitised by the ADCs showing the baseline and the pulse height.

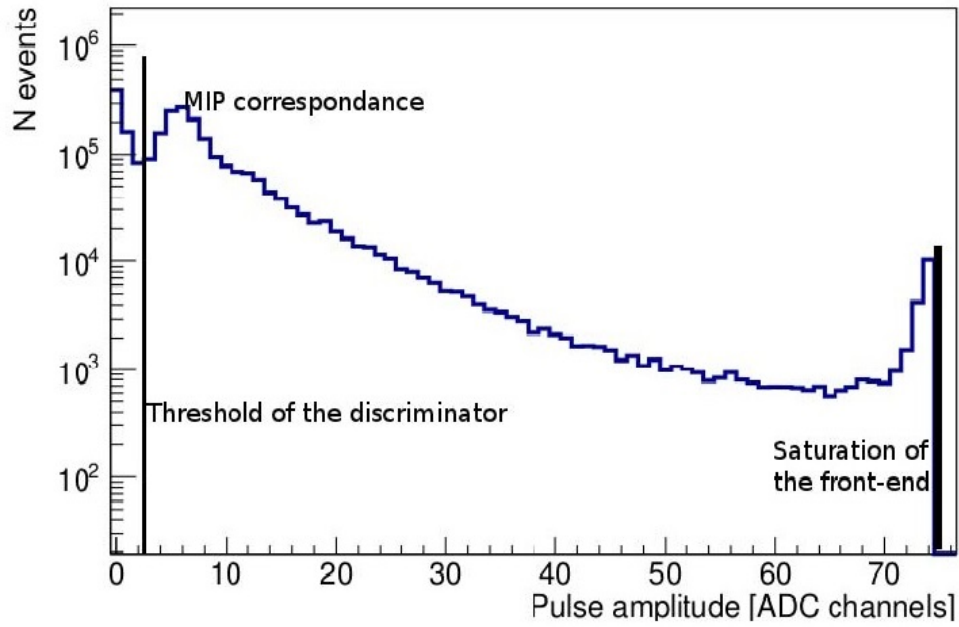


Figure 5: The amplitude spectrum of BCM1F measured with the ADCs during collisions.

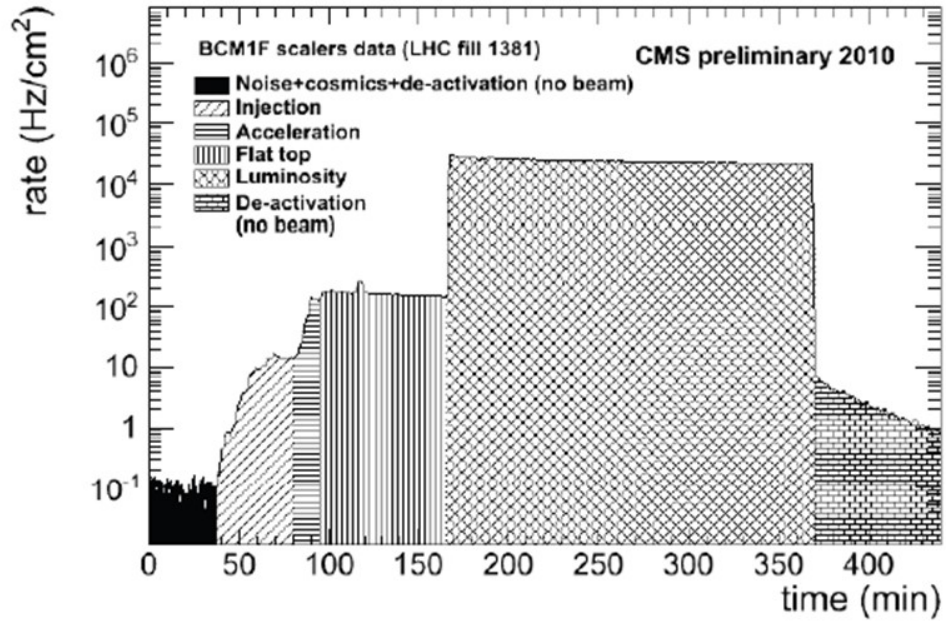


Figure 6: Hit rate with the scalars during an LHC fill.

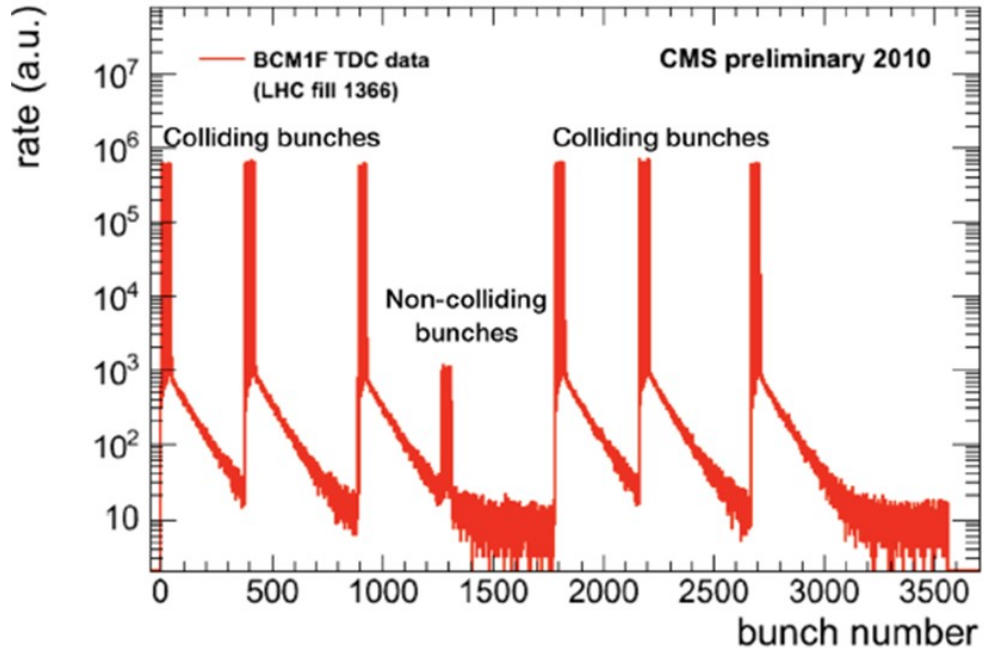


Figure 7: Hit rate as a function of time (in units of bunch numbers).

### 2.2.3 Luminosity Monitoring

The hit rate is very large during luminosity when the collisions take place (Figure 6). Those hits are essentially particles arising from the collisions, therefore, the rate should be proportional to the luminosity. It is very promising to use BCM1F as a luminosity monitoring tool as well for the CMS experiment.

### 2.2.4 Time Information

The discriminated analogue signals are digitized by a multi-hit TDC CAEN V767 board with 0.8 ns resolution. The clock signal of an LHC orbit is used as a trigger. The TDC then provide the time of the hits within an LHC orbit. This time can be converted into the bunch number following the LHC bunch numbering scheme, which permits an independent identification of each single bunch. An example of the arrival time distribution of particles within an orbit in an LHC is shown in Figure 7.

The time information can also be very useful for diagnostics of beam conditions identifying anomalous behavior of the beams or even of single bunched. The observation of different rates of non-colliding bunches with similar intensities, for instance, can be an indication of potential problems.

### 2.2.5 Albedo Effect

After the collision, long tails with exponential and constant shapes are observed in the rates from the TDCs and can be clearly seen in Figure 7. Simulations using the FLUKA Monte Carlo[7] describe well the shape of the hit rate distribution as a function of time when compared with the measured data (Figure 8)[8], and provide information about the particle contents of the albedo. The tails are mostly caused by neutrons, photons, electrons and positrons.

## 3 Relevant Physical Quantities in Simulation

### 3.1 Simulated Hits

In the simulation, once a particle come across the sensor and get felt by the sensor, what we call a hit generates. Nhits is the number of this kind of hits. For all the eight sensors, Nhits means the number of hits in whichever sensor the particles are felt. For each sensor, there are also quantities like Nhits but needed to be separated manually from the total Nhits.

### 3.2 Time of Flight

Time of flight means the time of the difference between the happen of the collision and the generation of one hit. The typical time of flight is about 6 ns because of the distance between IP and the sensor (1.8 m, Figure 2) and the velocity of relativistic particles. Time of Flight can be much greater than 6 ns for the albedos.



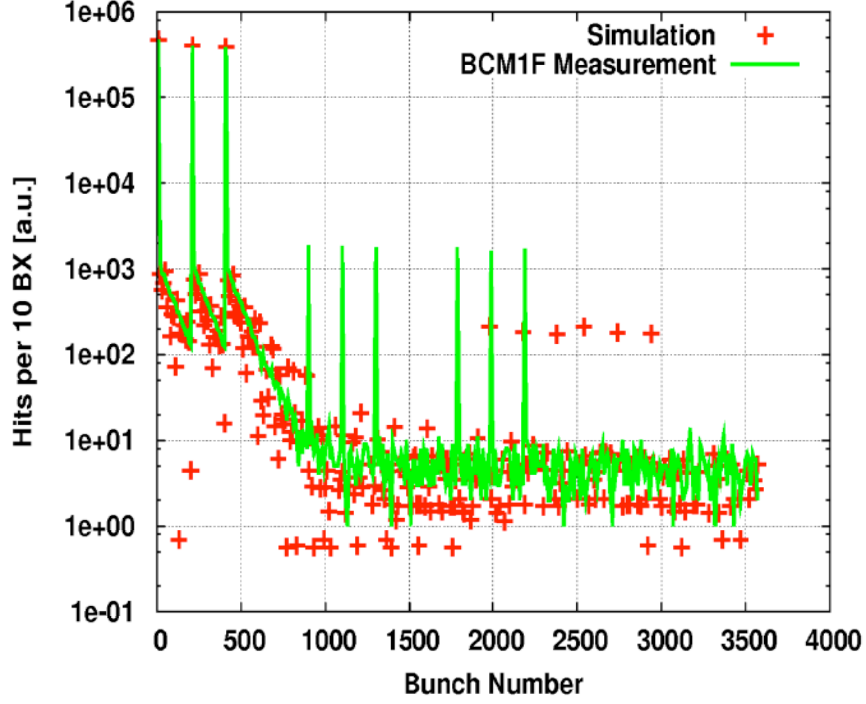


Figure 8: Comparison of the measured data and FLUKA.

### 3.3 Signal

Signal is the real source of the spectrum. When a particle passes by one sensor, a hit generates and is felt by the front-end. Then a signal, as Figure 4 shows, is created and transferred to the next process. And then the system will have a time about 10 ns, which is called dead time for the discriminator, to deal with the signal and record the information. During the dead time the sensor is "blind" for any other hit comes, no reaction will take place, which makes the statistic result of flight time significative.

### 3.4 Pile-up

Pile-up is the extra collisions for a bunch-crossing (BX). The number of pile-up equals to the result of the number of collisions minus one. When it comes larger, the difference between the number of collisions and pile-up is not obvious.

### 3.5 Hit Probability

Hit probability can be obtained by dividing the number of signal by the number of bunch crossing. The number of bunch crossing is the result of dividing the number of collisions by pile-up. Hit probability is very important to check whether the simulation is right and compare the different methods of simulation. Hit probability is the probability that a BCM1F channel will record a hit when a BX happens.

## 4 Processing Methods

### 4.1 Simulation Samples

The eight sensors are named sensor 11, sensor 12, sensor 13, sensor 14 on one side and sensor 21, sensor 22, sensor 23, sensor 24 on the other side in the simulation as Figure 9 shows.

Some settings for the BCM1F Monte Carlo samples in the simulation are shown in the following.

- Pythia Minimum Bias samples at 8 TeV, 1 M events.
- No pile-up simulated: one event = one collision.
- Pile-up emulated by accumulating consecutive events.
- BCM1F geometry of LHC Run 1 with 8 sensors.
- The real size for the sensor is  $4.7 \times 4.7 \times 0.5 \text{ mm}^3$  in the simulation.

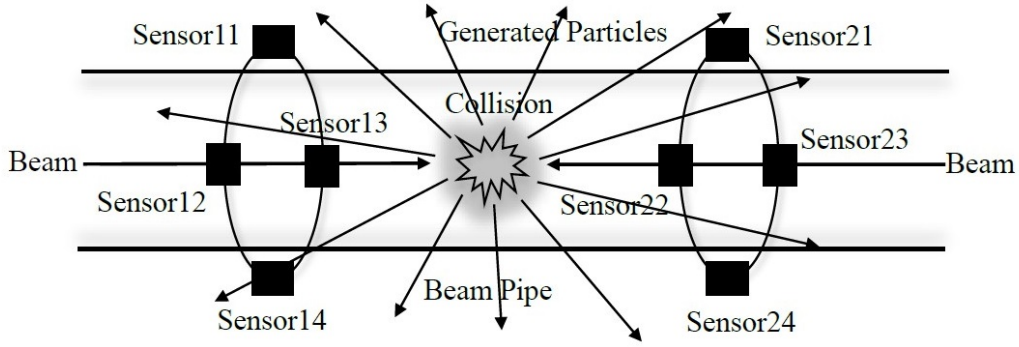


Figure 9: The name of the eight sensors in the simulation.

The geometric circumstances for the simulation are shown in Figure 10.

### 4.2 Luminosity Algorithms

For luminosity measurement some algorithms need to be processed.

- XOR+: Requires hits on the +z side and no hits on the -z side.
- XOR-: Requires hits on the -z side and no hits on the +z side.
- AND: Requires hits on both the +z and -z sides.
- OR: Requires hits on the +z or -z sides.

The OR is the one used for luminosity measurement so far.

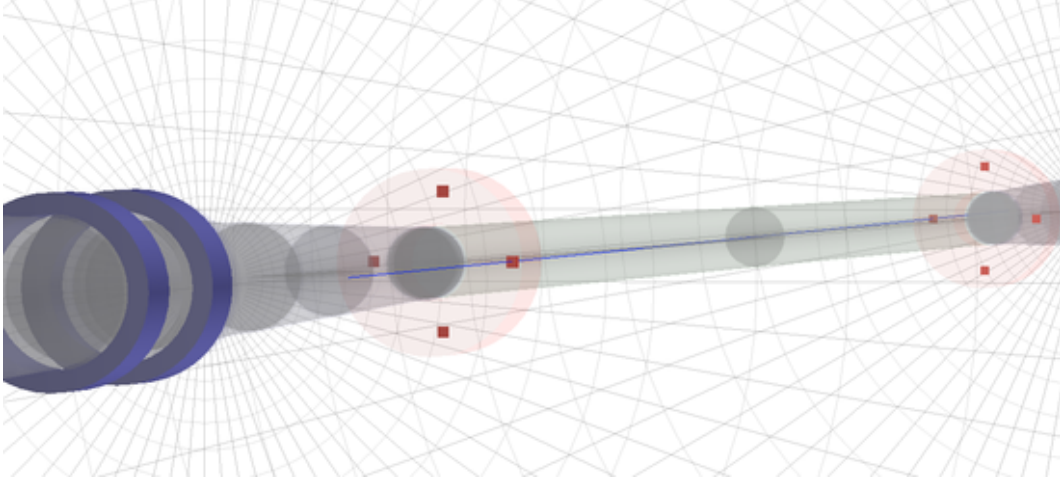


Figure 10: The geometry for the simulation.

### 4.3 Channel Splitting

To reduce the rate in each channel, each sensor is split into 2 channels for more studies using the same Monte Carlo simulation. As Figure 11 shows, each sensor has two channels that the left and right side both become a new independent channel. After splitting for each sensor, the new channels are named from 1 to 16 as Figure 12 shows. Then the same thing, signal collection, hit probability, luminosity algorithms, are processed for the new channels. The result in next section shows that splitting gives significant reduction of rate and better linearity of the plot for the hit probability depending on the pile-up.

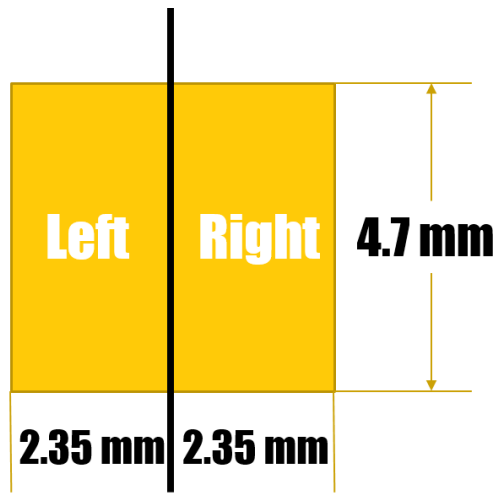


Figure 11: Channel splitting.

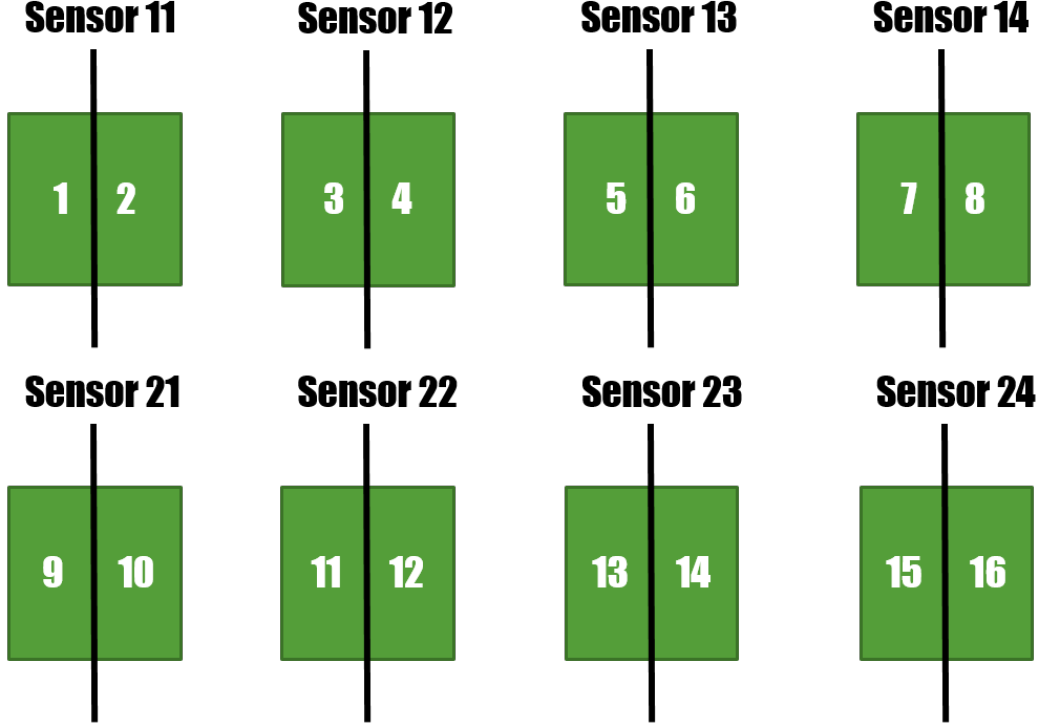


Figure 12: New channel ID numbers.

## 5 Results

### 5.1 Hit Probability

The Nhits for each sensor is calculated as a histogram with the macro as Figure 13 shows (sensor 11 to sensor 14).

To collect a signal, a new quantity called  $\Delta t$  is defined as the absolute of the difference between time of flight for two hits in one event. If there is less than 2 hits in one event, no count will be recorded. If there is more than 2 hits in one event, calculate  $\Delta t$  for every two hits. Then  $\Delta t$  is used to identify a signal: one signal has a dead time about 10 ns, no signals will be recorded after the 10 ns of one signal. An example of the histogram of signal depending on time is shown in Figure 14. The albedos can be seen clearly due to the log scaling axis. If the bunches come in a fixed period, the histogram will be discrete as Figure 15 shows.

The typical flight time is 6 ns, a time window between 6 ns and 10 ns is also used to collect the signals as sketched in Figure 16. (In Figure 16 the time window is between 5 ns to 7 ns.)

Hit probability depending on pile-up for the eight sensors is shown in Figure 17.

The data from measurement[9] also gives the plot of hit probability, whose comparison with the simulation is shown in Figure 18. The data is not corrected for inefficiency. Reasonable agreement can be found from the comparison.

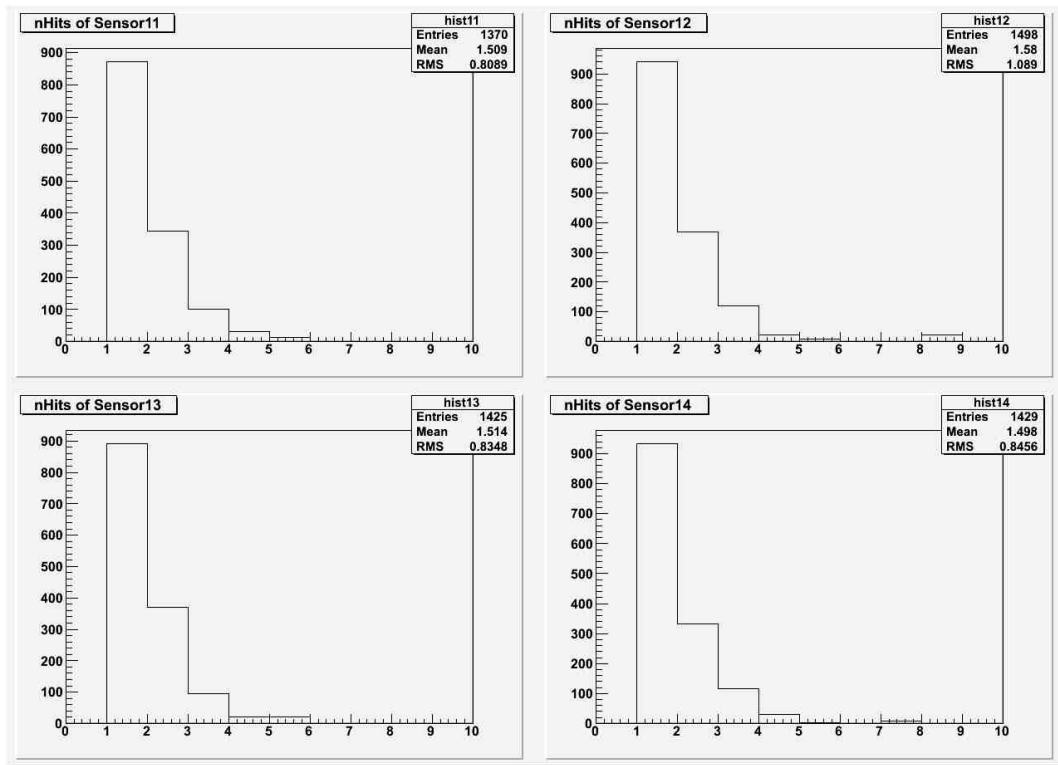


Figure 13: Histogram of the number of simulated hits for sensor 11 to sensor 14.

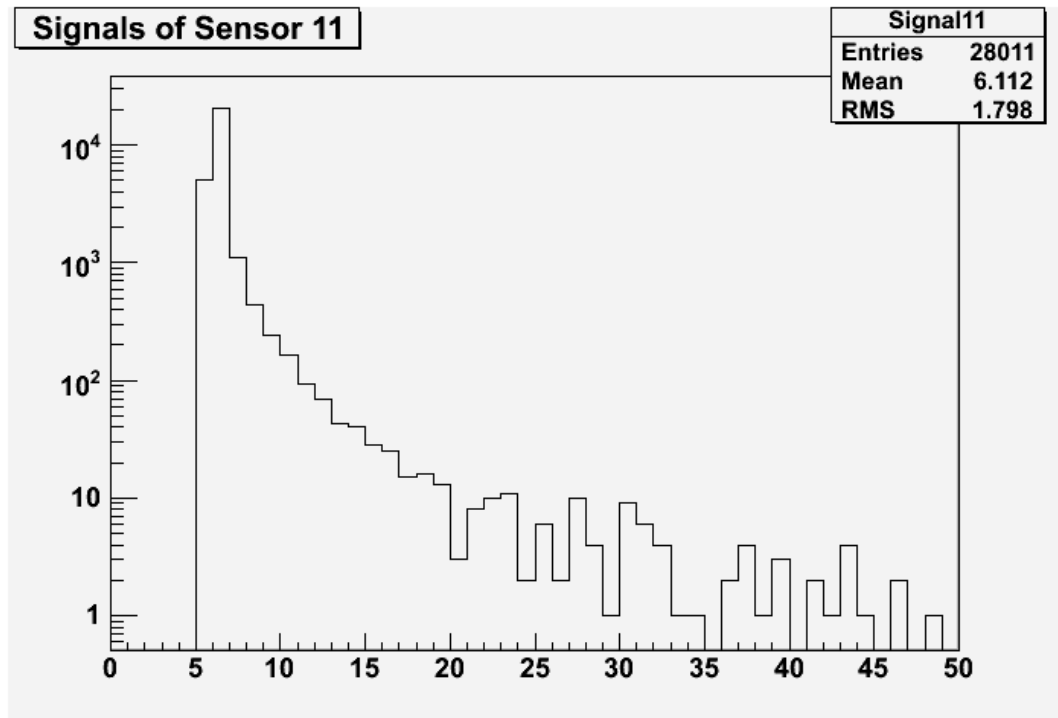


Figure 14: An example of the histogram of signal depending on time (ns).

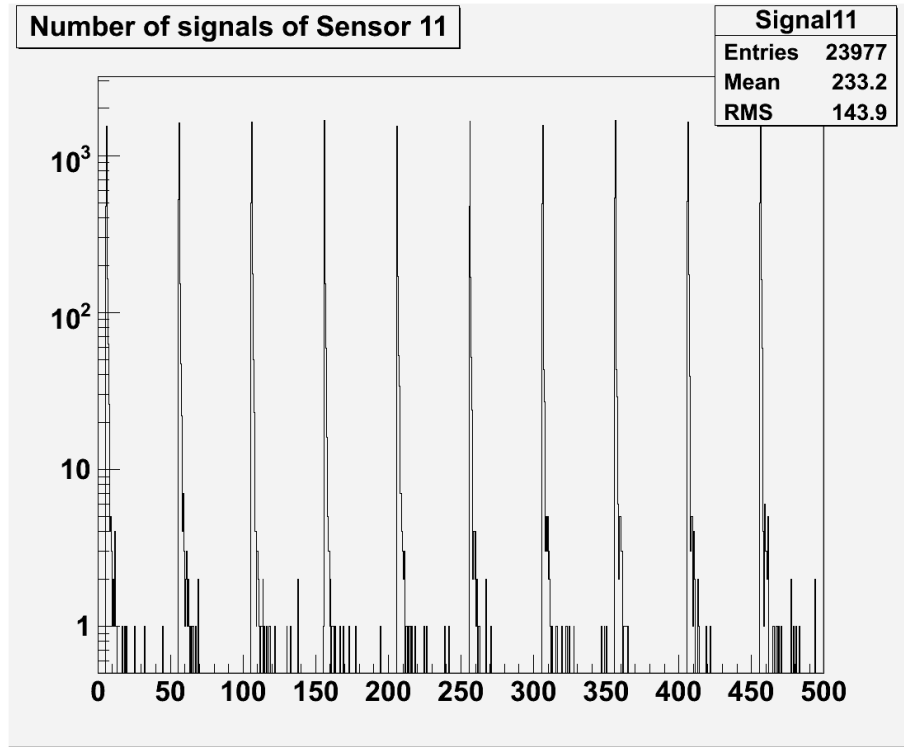


Figure 15: An example of histogram of signal depending on time when the bunches come in a fixed period.

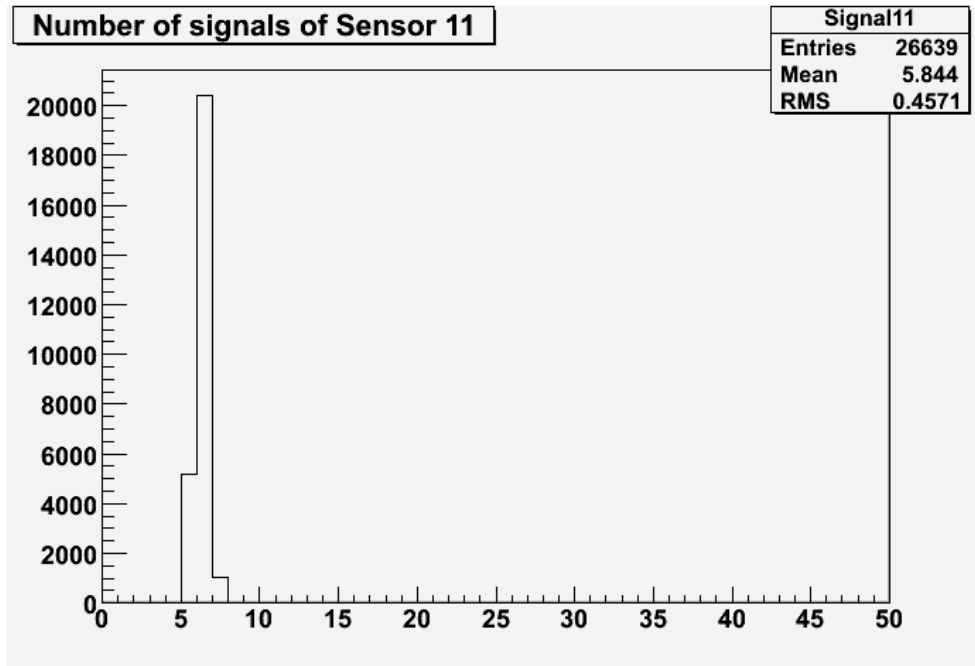


Figure 16: Histogram of signal with a time window between 5 ns to 7 ns.

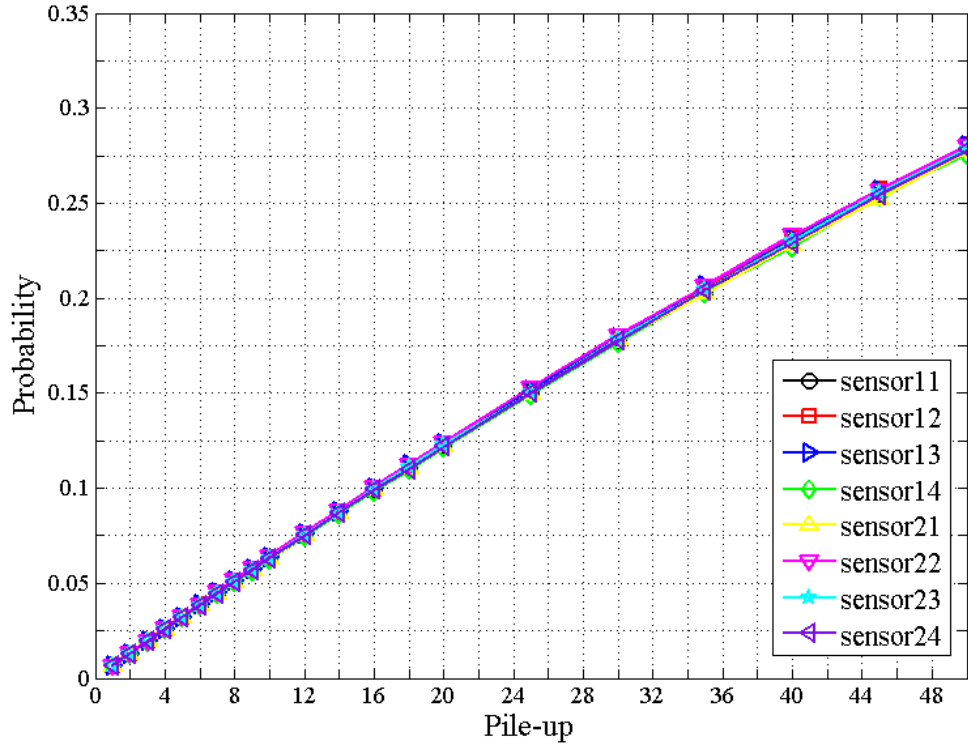


Figure 17: Hit probability depending on pile-up for the eight sensors.

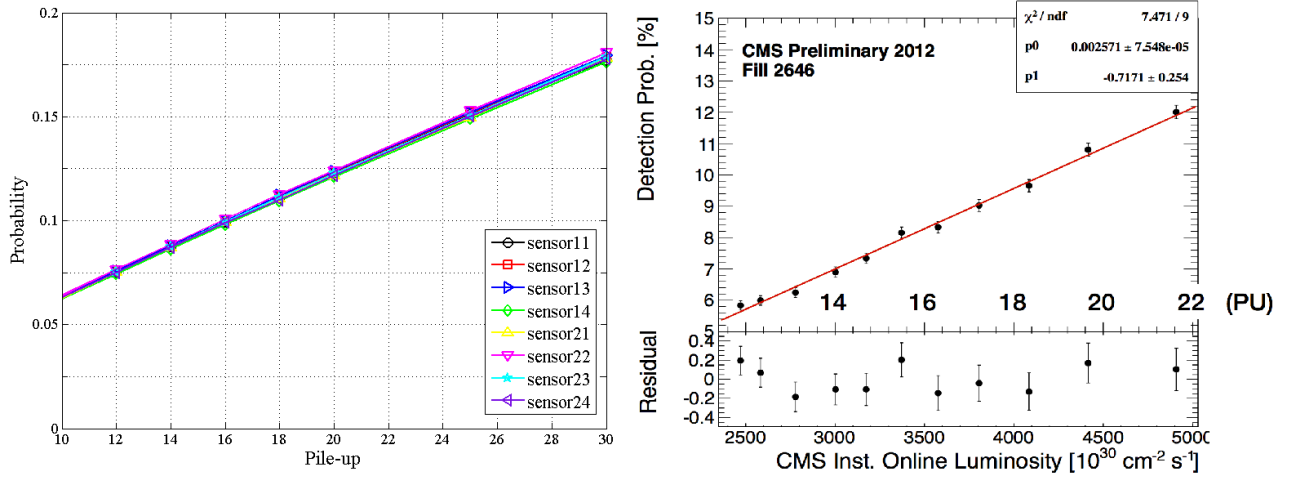


Figure 18: Comparison between the simulation and measurement data.

## 5.2 Luminosity Algorithms

Luminosity algorithms have been defined in the previous section. The OR counts can be divided into the other three categories: XOR+, XOR- and AND.

$$OR = XOR_+ + XOR_- + AND \quad (1)$$

This condition is always used to check the result. As stated, the OR is the one used for luminosity measurement so far. However, the OR has very large hit probability. The method is not appropriate for luminosity measurement when higher pile-up and rate. For the BRM group a rule of thumb is that the hit probability should not be greater than 75% for the luminosity measurement. The hit probability for the luminosity algorithms is shown in Figure 19.

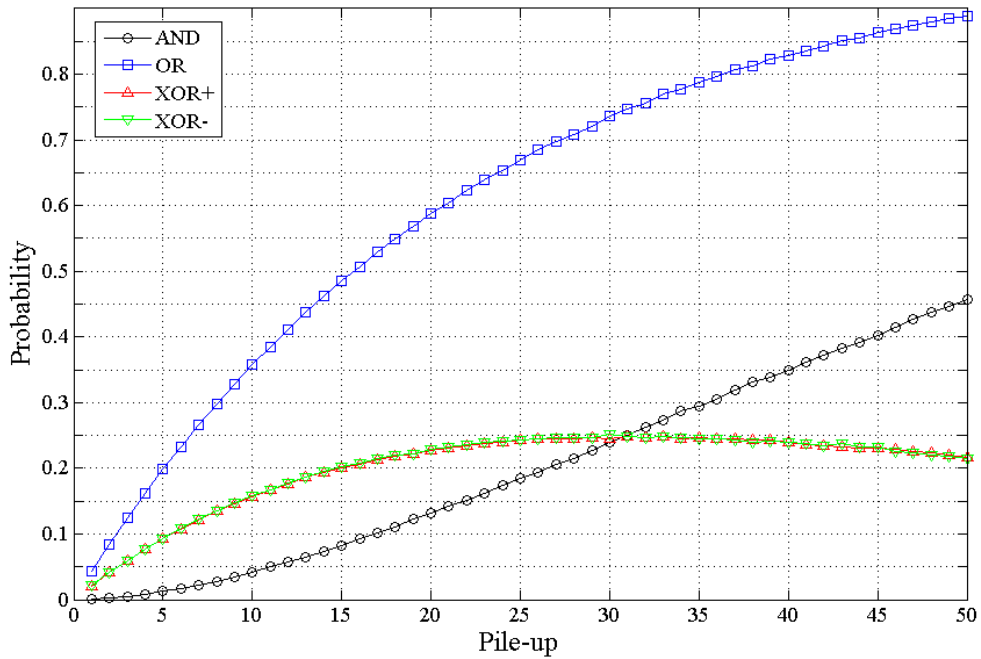


Figure 19: The hit probability for the luminosity algorithms.

## 5.3 Channel Splitting

The rate for each channel will reduce after splitting. The hit probability for each channel is shown in Figure 20. The average hit probability for +z side, -z side, odd channels, even channels and all channels is shown in Figure 21. From the plot a difference between the odd channels and the even channels can be found. But the reason is to be investigated from the simulation. Splitting channels give significant reduction of rate and better linearity, as sketched in Figure 22. The hit probability with the splitting channels is nearly the half of that with full sensors mainly due to the size of the sensor.



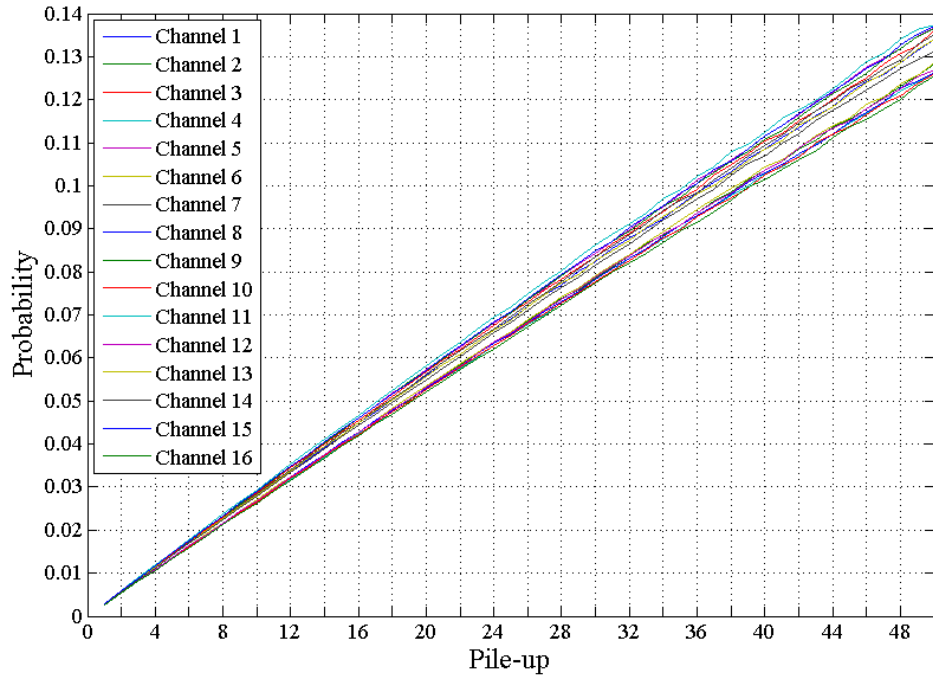


Figure 20: The hit probability for each channel.

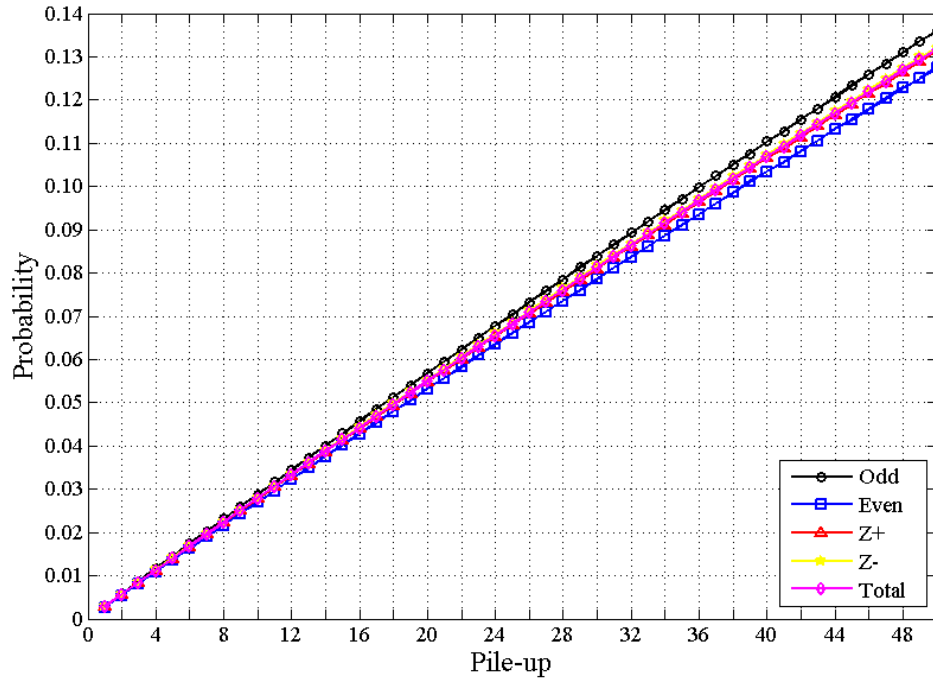


Figure 21: Average hit probability for some items.

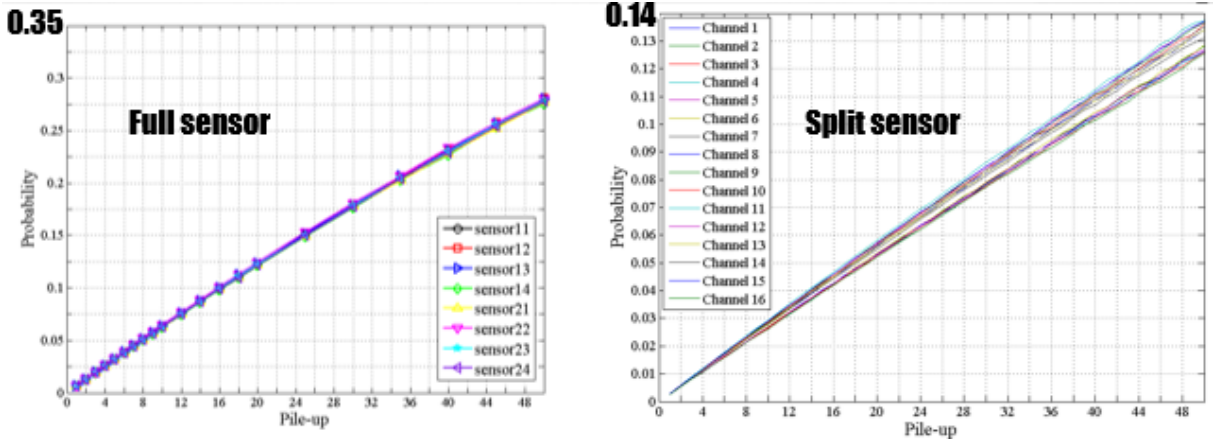


Figure 22: Comparison before and after splitting.

Luminosity algorithms are also processed for the splitting channels. The odd channels are grouped together for the luminosity algorithms and the same for the even channels. Each group has 8 channels as well as the previous result. The plot of hit probability for these algorithms is shown in Figure 23.

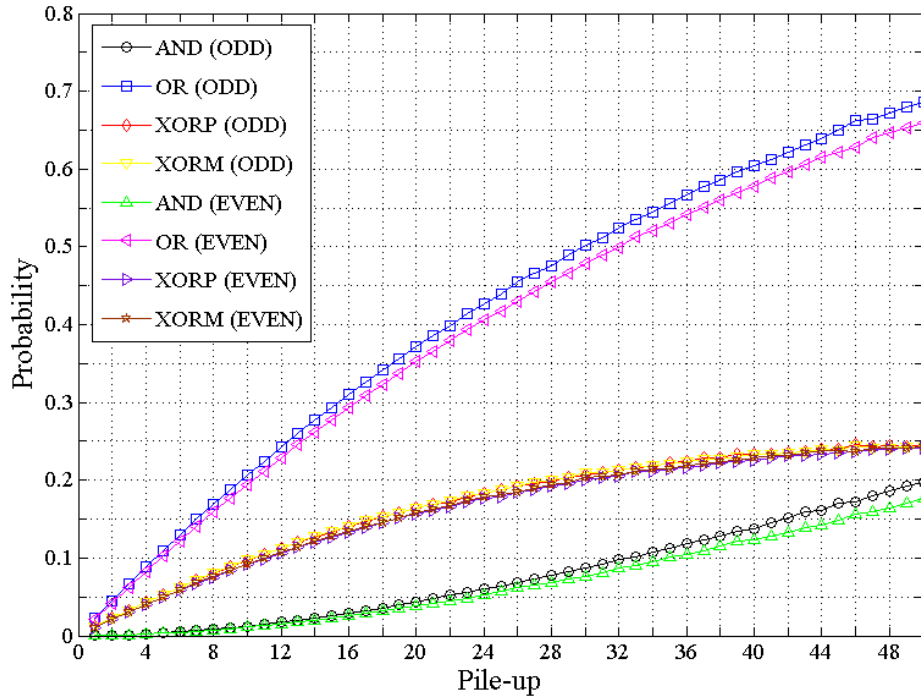


Figure 23: Hit probability for algorithms with splitting channels.

Comparison for the algorithms with splitting and full sensors can be done for further research as Figure 24, Figure 25 and Figure 26 show.

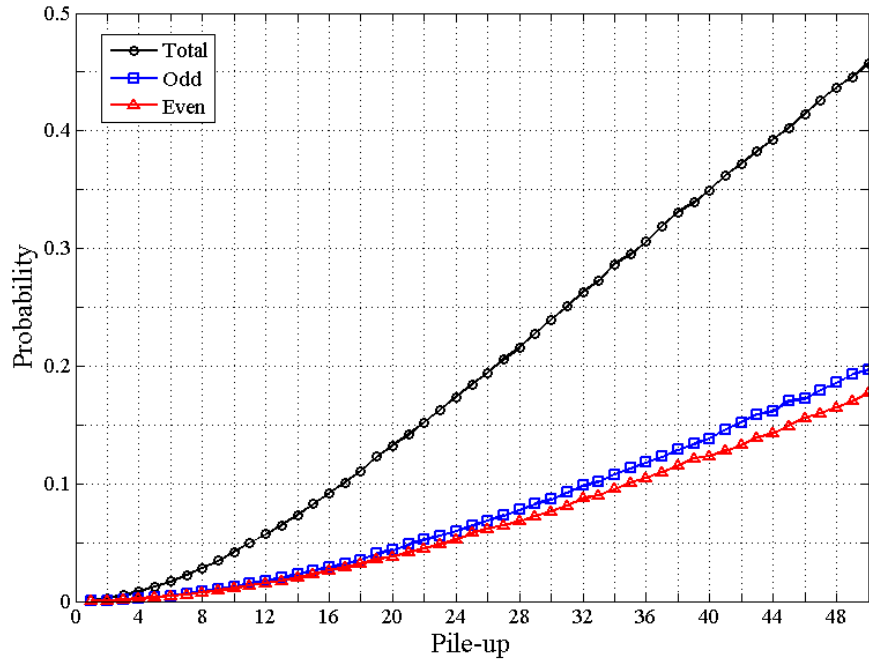


Figure 24: AND comparison before and after splitting.

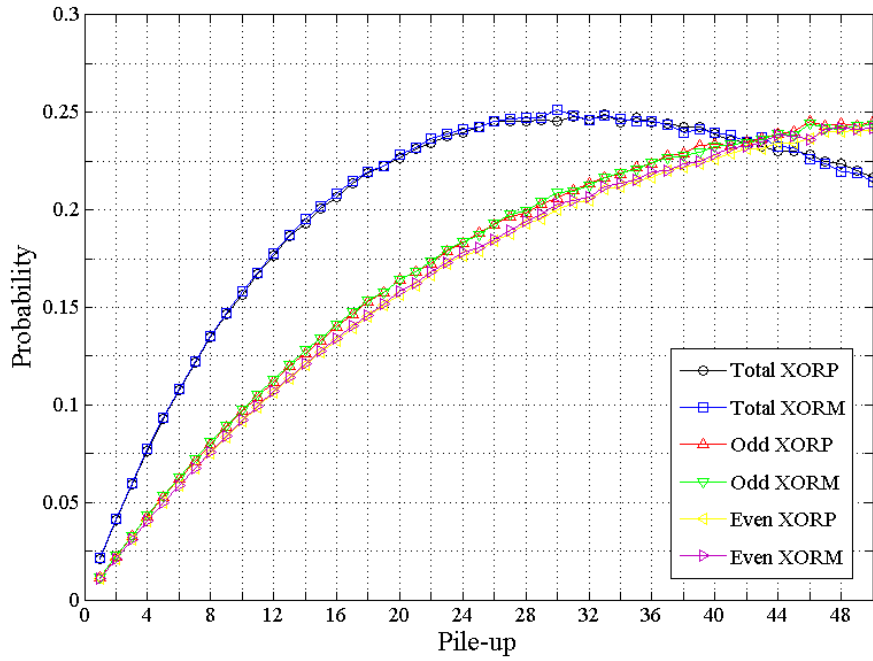


Figure 25: XOR comparison before and after splitting.

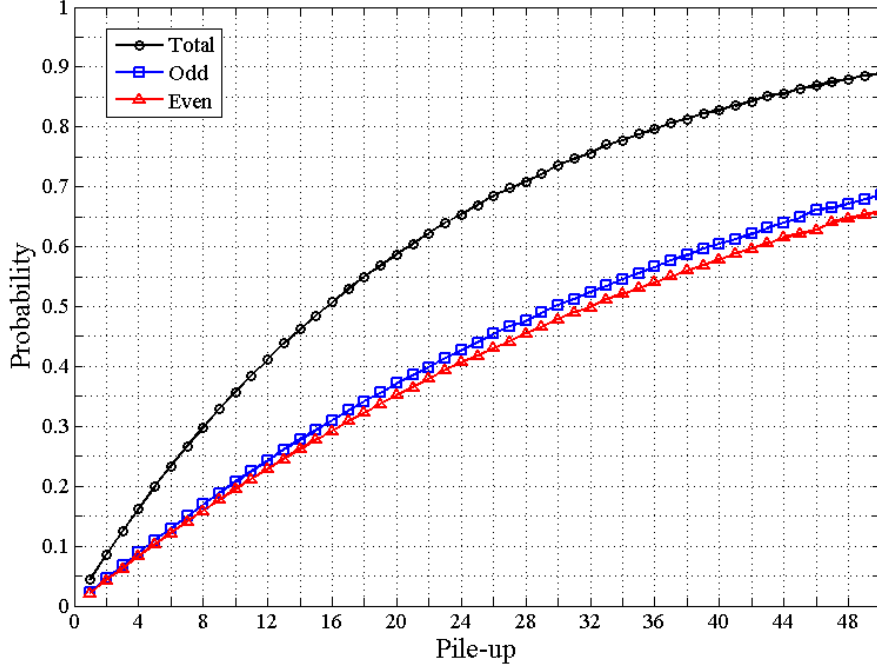


Figure 26: OR comparison before and after splitting.

Method is still valid for pile-up conditions larger than 50 for the OR algorithm with splitting sensors as Figure 26 shows, which will help the luminosity measurement.

## 6 Summary and Conclusions

As the previous statement shows, studies for luminosity measurement are performed with the upgraded CMS fast beam conditions monitor BCM1F using Monte Carlo simulations. The main idea is to collect the eligible signals and calculate the hit probability for different pile-up number and luminosity algorithms. The result of study shows that the single hit probability in the simulation reproduces the data. For further research about luminosity measurement, sensor splitting is processed and compared with the previous consequence. It is proved that the splitting of the sensor helps both reducing the rate and linearity.

## References

- [1] L. Evans, F.Bryant (Eds.), JINST, 3S08001 (2008)
- [2] S. Chatrchyan *et al.*, JINST, 3S08004 (2008)
- [3] A. Bell *et al.*, Nucl. Instr. and Meth. A614, 433 (2010)
- [4] L. Fernandez-Hernando *et al.*, Nucl. Instr. and Meth. A552, 183 (2005); A. Mcpherson, *Beam Condition Monitoring and radiation damage concerns of the experiment*, in: Proceedings LHC Project Workshop, Chamonix XV, 2006, p.198
- [5] R. Walsh, *Performance of the CMS Fast Beam Conditions Monitor*
- [6] N. Odell *et al.*, *The Compact Muon Solenoid Experiment Detector Note*
- [7] A. Ferrari *et al.*, CERN 2005-10 (2005)
- [8] S. Müller, *The Beam Condition Monitor 2 and the Radiation Environment of the CMS Detector at the LHC*, CERN-THESIS-2011-085, CMS-TS-2010-042
- [9] Internal communication